

# Joint Estimation of Carrier Offset and Code Timing for DS-CDMA With Performance Analysis

Khaled Amleh, *Member, IEEE*, and Hongbin Li, *Member, IEEE*

**Abstract**—This paper considers the problem of joint carrier offset and code timing estimation for code-division multiple-access (CDMA) systems. In contrast to existing schemes that require nonlinear iterative searches over the multidimensional parameter space, this paper proposes a blind estimator that provides an algebraic solution to the joint parameter estimation problem. By exploiting the subspace structure of the observed signal, the multiuser estimation is first decoupled into a series of single-user estimation problems, and then analytical tools of polynomial matrices are invoked for joint carrier and code timing estimation of a single user. The proposed estimator is near-far resistant. It can deal with frequency-selective and time-varying channels. The performance of the proposed scheme is examined analytically by a first-order perturbation analysis. The authors also derive an unconditional Cramér–Rao bound (CRB) that is conditioned neither on fading coefficients nor information symbols; as such, the CRB is considered a suitable lower bound for blind methods. Numerical examples are presented to evaluate and compare the proposed and a multidimensional search (MD-search)-based scheme.

**Index Terms**—Carrier offset and code timing estimation, code-division multiple access (CDMA), Cramér–Rao bound, perturbation analysis, time-selective and frequency-selective channels.

## I. INTRODUCTION

INITIAL spreading code and carrier frequency synchronization that precede symbol detection are challenging problems in direct-sequence code-division multiple-access (DS-CDMA) systems [1]. A conventional technique is to search serially through all potential code phases and frequencies for the desired user while treating the multiaccess interference (MAI) as noise [1, ch. 5]. This approach, albeit easy to implement, suffers the MAI, particularly in a near-far environment. A number of MAI-resistant code synchronization schemes have been introduced recently. These schemes can be classified as training-based methods (see [2], [3], and references therein), which require transmitting symbols known to the receiver, and blind techniques (e.g., [4]–[6] and references therein), which require no training but rely on some inherent structure of the transmitted signal.

Most of the above MAI-resistant acquisition schemes consider only code synchronization, assuming that carrier synchroni-

zation has been achieved at a prior stage. There are limited studies on joint code and frequency synchronization. One example is a joint carrier offset and code timing estimator proposed in [7], where frequency-nonselective and time-invariant channels were considered. This estimator involves nonlinear iterative searches over the multidimensional parameter space. It is computationally involved and requires accurate initial parameter estimates that are often difficult to obtain.

The authors present herein an algebraic approach to joint carrier offset and code timing estimation in CDMA systems. To some extent, the proposed method is reminiscent of a technique proposed in [8] for joint channel and carrier offset estimation. However, there are notable distinctions. One is that [8] assumes a strictly quasi-synchronous system in which intersymbol interference (ISI)-free chip samples are available. It was also assumed that there is a finite-duration impulse response (FIR) channel model with time-invariant and congruent channel taps. The authors relax these assumptions to allow for channel variations and adjacent-symbol ISI (no ISI-free chips are available); the path delays are otherwise unrestricted. Specifically, by exploiting the subspace structure of the observed signal, the multiuser estimation is first decoupled into a series of single-user estimation problems. Next, analytical tools of polynomial matrices are utilized for joint carrier and code timing estimation of a single user. The proposed estimator is near-far resistant. It can deal with frequency-selective and time-varying channels. The performance of the proposed scheme is examined analytically by a first-order perturbation analysis. An unconditional Cramér–Rao bound (CRB) that is conditioned on neither fading coefficients nor information symbols was also derived. Hence, CRB is considered a more suitable lower bound than a conditioned CRB (e.g., [4]) for blind code timing estimators. Numerical examples are presented to evaluate and compare the proposed and a multidimensional search (MD-search)-based schemes.

*Notation:* Vectors (matrices) are denoted by boldface lower (upper) case letters; all vectors are column vectors; superscripts  $(\cdot)^*$ ,  $(\cdot)^T$ ,  $(\cdot)^H$ , and  $(\cdot)^\dagger$  denote the complex conjugate, transpose, conjugate transpose, and Moore–Penrose pseudo-inverse, respectively;  $\mathbf{I}_N$  denotes the  $N \times N$  identity matrix;  $\mathbf{0}$  denotes an all-zero vector/matrix;  $\|\cdot\|$  denotes the vector 2-norm;  $E\{\cdot\}$  denotes the statistical expectation;  $\text{diag}\{\cdot\}$  denotes a diagonal or block diagonal matrix; and  $\text{null}(\mathbf{A})$  denotes the null space of matrix  $\mathbf{A}$ .

## II. PROBLEM FORMULATION

Consider a baseband asynchronous  $K$ -user DS-CDMA system. The transmitted signal for user  $k$  is given by  $s_k(t) =$

Manuscript received May 12, 2003; revised December 9, 2003 and September 7, 2004; accepted September 13, 2004. The editor coordinating the review of this paper and approving it for publication is Q. Bi. This work was supported in part by the NSF under Grant CCF-0514938, in part by the ARO under Grant DAAD19-03-1-0184, and in part by the AFRL under Grant FA8750-05-2-0001.

K. Amleh is with the Engineering Department, Penn State University at Mont Alto, Mont Alto, PA 17237 USA (e-mail: kaa13@psu.edu).

H. Li is with the Department of Electrical and Computer Engineering, Stevens Institute of Technology, Hoboken, NJ 07030 USA (e-mail: hli@stevens.edu).

Digital Object Identifier 10.1109/TWC.2005.853819

$\sum_{m=0}^{M-1} d_k(m)\pi_k(t - mT_s)$ , where  $M$  is the number of symbols used for synchronization,  $d_k(m)$  and  $\pi_k(t)$  denote the  $m$ th symbol and spreading waveform, respectively, for user  $k$ , and  $T_s = NT_c$  denotes the symbol interval, with  $T_c$  and  $N$  being the chip interval and spreading gain, respectively. The signal  $s_k(t)$  passes through a baseband frequency-selective time-varying channel. The received signal is given by

$$y(t) = \sum_{k=1}^K \sum_{l=1}^{L_k} \alpha_{k,l}(t) s_k(t - \tau_{k,l}) e^{j\Omega_k(t - \tau_{k,l})} + n(t) \quad (1)$$

where  $L_k$  is the number of paths for user  $k$ ,  $\Omega_k$  is the frequency offset,  $\alpha_{k,l}(t)$  is the fading coefficient for the  $l$ th path,  $\tau_{k,l}$  is the associated delay, and  $n(t)$  is the channel noise with zero-mean and variance  $\sigma_n^2$ . To avoid ambiguity, the authors assume that the delay for the desired user is such that  $\tau_{k,l} < T_s$ . This could be due to a prior coarse synchronization that pulls the timing uncertainty to within a symbol interval (e.g., [2]). On the other hand, if  $\tau_{k,l} \geq T_s$ , the proposed blind scheme can identify the fractional delay, i.e.,  $\tau_{k,l} \bmod T_s$ ; the integer portion of the delay cannot be identified blindly. In what follows, the authors also assume that the time-varying fading coefficient  $\alpha_{k,l}(t)$  is a stationary random process while the number of paths  $L_k$  and path delay  $\tau_{k,l}$  remain (approximately) fixed during acquisition. The receiver front-end is a chip-matched filter (CMF) that outputs samples  $y(l) = y(t)|_{t=lT_i}$ , where  $T_i = T_c/Q$  is the sampling interval, with  $Q \geq 1$  denoting the oversampling factor (an integer). It is convenient to write  $\tau_{k,l}$  as a multiple of the sampling interval  $T_i$

$$\tau_{k,l} = (p_{k,l} + \mu_{k,l})T_i$$

where  $p_{k,l} \in [0, NQ - 1]$  denotes the integer delay while  $\mu_{k,l} \in [0, 1)$  is the fractional delay.

Let  $\mathbf{y}(m) \triangleq [y(mNQ), \dots, y(mNQ + NQ - 1)]^T$  and  $\mathbf{c}_k \triangleq [c_k(0), \dots, c_k(NQ - 1)]^T$ , where  $c_k(n) = (1/T_i) \int_{(n-1)T_i}^{nT_i} \pi_k(t) dt$ . Due to asynchronous transmissions, two adjacent symbols in each path contribute to  $\mathbf{y}(m)$ . As a result,  $\mathbf{y}(m)$  can be expressed as [5]<sup>1</sup>

$$\mathbf{y}(m) = \sum_{k=1}^K \boldsymbol{\Sigma}_k(\omega_k) \mathbf{A}_k(\boldsymbol{\tau}_k) \boldsymbol{\beta}_k(m) + \mathbf{n}(m), \quad m = 0, 1, \dots, M - 1 \quad (2)$$

<sup>1</sup>The authors invoke the standard assumption that the frequency offset is small compared to the chip rate, i.e.,  $\Omega_k \ll 1/T_c$ , so that the exponential term in (1) remains approximately constant within  $T_i$  [8]. Also, to simplify the data model, the channel is assumed to remain unchanged within one  $T_s$  and  $\alpha_{k,l}(m) \triangleq \alpha_{k,l}(t)|_{t=mT_s}$ . In testing the proposed scheme, the authors allow  $\alpha_{k,l}(t)$  to vary continuously according to a more realistic channel model; see Section VI.

where  $\omega_k \triangleq \Omega_k T_i$  denotes the normalized carrier offset

$$\boldsymbol{\tau}_k \triangleq [\tau_{k,1}, \dots, \tau_{k,L_k}]^T$$

$$\boldsymbol{\Sigma}_k(\omega_k) \triangleq \text{diag} \left\{ 1, e^{j\omega_k}, \dots, e^{j\omega_k(NQ-1)} \right\}$$

$$\boldsymbol{\beta}_k(m) \triangleq [\beta_{k,1}(m), \bar{\beta}_{k,1}(m), \dots, \beta_{k,L_k}(m), \bar{\beta}_{k,L_k}(m)]^T$$

$$\beta_{k,l}(m) \triangleq \alpha_{k,l}(m) d_k(m-1) e^{j\omega_k \left( \frac{mNQ - \tau_{k,l}}{T_i} \right)}$$

$$\bar{\beta}_{k,l}(m) \triangleq \alpha_{k,l}(m) d_k(m) e^{j\omega_k \left( \frac{mNQ - \tau_{k,l}}{T_i} \right)}$$

and  $\mathbf{n}(m)$  denotes the  $NQ \times 1$  channel noise vector. The spreading code matrix  $\mathbf{A}_k(\boldsymbol{\tau}_k)$  is given by

$$\mathbf{A}_k(\boldsymbol{\tau}_k) = [\mathbf{a}_k(\tau_{k,1}), \bar{\mathbf{a}}_k(\tau_{k,1}), \dots, \mathbf{a}_k(\tau_{k,L_k}), \bar{\mathbf{a}}_k(\tau_{k,L_k})] \quad (3)$$

where  $\mathbf{a}_k(\tau_{k,l})$  and  $\bar{\mathbf{a}}_k(\tau_{k,l})$  are formed from the acyclic left right shift of the spreading code  $\mathbf{c}_k$  [5]

$$\mathbf{a}_k(\tau_{k,l}) \triangleq (1 - \mu_{k,l}) \mathbf{c}_k^l(p_{k,l}) + \mu_{k,l} \mathbf{c}_k^l(p_{k,l} + 1) \quad (4)$$

$$\bar{\mathbf{a}}_k(\tau_{k,l}) \triangleq (1 - \mu_{k,l}) \mathbf{c}_k^r(p_{k,l}) + \mu_{k,l} \mathbf{c}_k^r(p_{k,l} + 1) \quad (5)$$

$$\mathbf{c}_k^l(p_{k,l}) \triangleq \mathbf{P}(p_{k,l}) \mathbf{c}_k$$

$$\mathbf{c}_k^r(p_{k,l}) \triangleq \bar{\mathbf{P}}(p_{k,l}) \mathbf{c}_k \quad (6)$$

where  $\mathbf{P}(p)$  and  $\bar{\mathbf{P}}(p)$  are shifting matrices

$$\mathbf{P}(p) \triangleq \begin{bmatrix} \mathbf{0} & \mathbf{I}_p \\ \mathbf{0} & \mathbf{0} \end{bmatrix}, \quad \bar{\mathbf{P}}(p) \triangleq \begin{bmatrix} \mathbf{0} & \mathbf{0} \\ \mathbf{I}_{NQ-p} & \mathbf{0} \end{bmatrix}. \quad (7)$$

Let

$$\mathbf{F}_k(p_{k,l}) \triangleq [\mathbf{P}(p_{k,l}) \mathbf{c}_k, \mathbf{P}(p_{k,l} + 1) \mathbf{c}_k]$$

$$\bar{\mathbf{F}}_k(p_{k,l}) \triangleq [\bar{\mathbf{P}}(p_{k,l}) \mathbf{c}_k, \bar{\mathbf{P}}(p_{k,l} + 1) \mathbf{c}_k]$$

$$\boldsymbol{\mu}_{k,l} \triangleq [1 - \mu_{k,l}, \mu_{k,l}]^T.$$

Then,  $\mathbf{a}_k(\tau_{k,l})$  and  $\bar{\mathbf{a}}_k(\tau_{k,l})$  can be compactly expressed as

$$\mathbf{a}_k(\tau_{k,l}) = \mathbf{F}_k(p_{k,l}) \boldsymbol{\mu}_{k,l}, \quad \bar{\mathbf{a}}_k(\tau_{k,l}) = \bar{\mathbf{F}}_k(p_{k,l}) \boldsymbol{\mu}_{k,l}. \quad (8)$$

The problem of interest is to estimate the code timing  $\{\boldsymbol{\tau}_k\}_{k=1}^K$  and the carrier frequency offset  $\{\omega_k\}_{k=1}^K$  from the received data  $\{\mathbf{y}(m)\}_{m=0}^{M-1}$  without any knowledge of the information symbols.

### III. JOINT CARRIER OFFSET AND CODE TIMING ESTIMATION

The proposed scheme is a subspace-based approach that decouples the multiuser parameter estimation problem into a series of single-user estimation. For ease of presentation, the authors first consider the noise-free case in Section III-A and then discuss the noisy case in Section III-B.

### A. Noise-Free Case

Let

$$\mathbf{x}(m) = \Theta(\omega)\mathcal{A}(\boldsymbol{\tau})\boldsymbol{\beta}(m)$$

where

$$\begin{aligned}\Theta(\omega) &\triangleq [\boldsymbol{\Sigma}_1(\omega_1), \dots, \boldsymbol{\Sigma}_K(\omega_K)] \\ \mathcal{A}(\boldsymbol{\tau}) &\triangleq \text{diag}\{\mathbf{A}_1(\boldsymbol{\tau}_1), \dots, \mathbf{A}_K(\boldsymbol{\tau}_K)\} \\ \boldsymbol{\tau} &\triangleq [\boldsymbol{\tau}_1^T, \dots, \boldsymbol{\tau}_K^T]^T \\ \boldsymbol{\beta}(m) &\triangleq [\boldsymbol{\beta}_1^T(m), \dots, \boldsymbol{\beta}_K^T(m)]^T.\end{aligned}$$

Let

$$\mathbf{X} \triangleq [\mathbf{x}(0), \dots, \mathbf{x}(M-1)]$$

that can be expressed as

$$\mathbf{X} = \Theta(\omega)\mathcal{A}(\boldsymbol{\tau})\mathbf{B}$$

where  $\mathbf{B} = [\boldsymbol{\beta}(0), \dots, \boldsymbol{\beta}(M-1)]$ . Let  $L \triangleq \sum_{k=1}^K L_k$  denote the total number of paths of all  $K$  users. The authors assume that  $NQ > 2L$  so that matrix  $\Theta(\omega)\mathcal{A}(\boldsymbol{\tau})$  is tall with full column rank, which is in general satisfied with independent spreading codes for different users and distinct path delays (of any one particular user). Furthermore, the authors assume that  $M > 2L$  and that  $\mathbf{B}$  has full row rank, which is again satisfied with independent data symbols for different users and independent or correlated (but not fully coherent) path gains (of any one particular user). With such assumptions, the singular value decomposition (SVD) can be expressed as

$$\mathbf{X} = [\mathbf{U}_s \quad \mathbf{U}_n] \begin{bmatrix} \boldsymbol{\Lambda}_{2L \times 2L} & \mathbf{0}_{2L \times (M-2L)} \\ \mathbf{0}_{(NQ-2L) \times 2L} & \mathbf{0}_{(NQ-2L) \times (M-2L)} \end{bmatrix} \begin{bmatrix} \mathbf{V}_s^H \\ \mathbf{V}_n^H \end{bmatrix} \quad (9)$$

where  $\boldsymbol{\Lambda}$  is a  $2L \times 2L$  diagonal matrix made from  $2L$  nonzero singular values and the associated left and right singular vectors are contained in  $\mathbf{U}_s \in \mathbb{C}^{NQ \times 2L}$  and  $\mathbf{V}_s \in \mathbb{C}^{M \times 2L}$ , respectively. It is ready to show that

$$\mathbf{U}_n^H \boldsymbol{\Sigma}_k(\omega_k) \mathbf{A}_k(\boldsymbol{\tau}_k) = \mathbf{0}, \quad k = 1, \dots, K. \quad (10)$$

Estimates of  $\omega_k$  and  $\boldsymbol{\tau}_k$  can be obtained from the above equations through nonlinear searches over an  $(L_k + 1)$ -dimensional parameter space, which are computationally involved and may suffer local convergence.

To seek an alternative solution, by which frequency offset and code timing can be estimated algebraically, the authors invoke the theory of polynomial matrices (e.g., [9]). For the  $l$ th path of user  $k$ , (10) is equivalent to (the authors henceforth drop the subscripts  $k$  and  $l$  for notational brevity)

$$\mathbf{U}_n^H \boldsymbol{\Sigma}(\omega) \mathbf{a}(\boldsymbol{\tau}) = \mathbf{0}, \quad \mathbf{U}_n^H \boldsymbol{\Sigma}(\omega) \bar{\mathbf{a}}(\boldsymbol{\tau}) = \mathbf{0}. \quad (11)$$

Let  $\tau \triangleq (p + \mu)T_i$  and  $z \triangleq e^{j\omega}$ . The authors may write  $\boldsymbol{\Sigma}(z) = \text{diag}\{1, z, \dots, z^{NQ-1}\}$ . Substituting (8) into (11) yields

$$\boldsymbol{\Psi}(z)\boldsymbol{\mu} = \mathbf{0}, \quad \bar{\boldsymbol{\Psi}}(z)\boldsymbol{\mu} = \mathbf{0} \quad (12)$$

where  $\boldsymbol{\Psi}(z) \triangleq \mathbf{U}_n^H \boldsymbol{\Sigma}(z) \mathbf{F}(p)$  and  $\bar{\boldsymbol{\Psi}}(z) \triangleq \mathbf{U}_n^H \boldsymbol{\Sigma}(z) \bar{\mathbf{F}}(p)$ . Notice that  $\boldsymbol{\Psi}(z)$  and  $\bar{\boldsymbol{\Psi}}(z)$  are  $(NQ - 2L) \times 2$  polynomial matrices in  $z$  of order  $NQ - 1$ . To see this, let  $\mathbf{u}_{n,i}$ ,  $\mathbf{f}_i^H(p)$ , and  $\bar{\mathbf{f}}_i^H(p)$ ,  $i = 1, 2, \dots, NQ$ , denote the  $i$ th column of  $\mathbf{U}_n^H$ , the  $i$ th row of  $\mathbf{F}(p)$ , and the  $i$ th row of  $\bar{\mathbf{F}}(p)$ , respectively. Then, the polynomial matrices  $\boldsymbol{\Psi}(z)$  and  $\bar{\boldsymbol{\Psi}}(z)$  can then be explicitly expressed as

$$\boldsymbol{\Psi}(z) = \sum_{i=1}^{NQ} \mathbf{u}_{n,i} \mathbf{f}_i^H(p) z^{i-1}, \quad \bar{\boldsymbol{\Psi}}(z) = \sum_{i=1}^{NQ} \mathbf{u}_{n,i} \bar{\mathbf{f}}_i^H(p) z^{i-1}. \quad (13)$$

Represent  $\boldsymbol{\Psi}(z)$  and  $\bar{\boldsymbol{\Psi}}(z)$  explicitly using column polynomial vectors

$$\boldsymbol{\Psi}(z) = [\boldsymbol{\psi}_1(z), \boldsymbol{\psi}_2(z)], \quad \bar{\boldsymbol{\Psi}}(z) = [\bar{\boldsymbol{\psi}}_1(z), \bar{\boldsymbol{\psi}}_2(z)].$$

Equation (12) implies that at the true values of  $p$  and the carrier offset,  $\boldsymbol{\psi}_1(z)$  and  $\boldsymbol{\psi}_2(z)$  are linearly dependent on each other, and so are  $\bar{\boldsymbol{\psi}}_1(z)$  and  $\bar{\boldsymbol{\psi}}_2(z)$ ; furthermore,  $\boldsymbol{\mu}$  lies in both  $\text{null}(\boldsymbol{\Psi}(z))$  and  $\text{null}(\bar{\boldsymbol{\Psi}}(z))$ .<sup>2</sup> Therefore, the rank of  $\text{null}(\boldsymbol{\Psi}(z))$  and  $\text{null}(\bar{\boldsymbol{\Psi}}(z))$  is one. Hence, the authors can construct projection matrices  $\mathbf{P}_{\boldsymbol{\psi}_2}^\perp(z)$  and  $\bar{\mathbf{P}}_{\bar{\boldsymbol{\psi}}_2}^\perp(z)$  that project to the orthogonal complement of vectors  $\boldsymbol{\psi}_2$  and  $\bar{\boldsymbol{\psi}}_2$ , respectively

$$\mathbf{P}_{\boldsymbol{\psi}_2}^\perp(z) \boldsymbol{\psi}_1(z) = \mathbf{0}, \quad \bar{\mathbf{P}}_{\bar{\boldsymbol{\psi}}_2}^\perp(z) \bar{\boldsymbol{\psi}}_1(z) = \mathbf{0}. \quad (14)$$

To construct  $\mathbf{P}_{\boldsymbol{\psi}_2}^\perp(z)$  and  $\bar{\mathbf{P}}_{\bar{\boldsymbol{\psi}}_2}^\perp(z)$ , it is noted that by the Bezout identity [9, p. 379] (see also [8]), there exist  $1 \times (NQ - 2L)$  polynomial vectors  $\mathbf{g}^H(z)$  and  $\bar{\mathbf{g}}^H(z)$  such that

$$\mathbf{g}^H(z) \boldsymbol{\psi}_2(z) = z^{-n_0}, \quad \bar{\mathbf{g}}^H(z) \bar{\boldsymbol{\psi}}_2(z) = z^{-\bar{n}_0} \quad (15)$$

for some appropriate delays  $n_0$  and  $\bar{n}_0$ ; see Appendix A for how to construct  $\mathbf{g}^H(z)$  and  $\bar{\mathbf{g}}^H(z)$ . Once the authors have these vectors,  $\mathbf{P}_{\boldsymbol{\psi}_2}^\perp(z)$  can be formed as

$$\mathbf{P}_{\boldsymbol{\psi}_2}^\perp(z) = z^{-n_0} \mathbf{I}_{NQ-2L} - \boldsymbol{\psi}_2(z) \mathbf{g}^H(z). \quad (16)$$

Likewise,  $\bar{\mathbf{P}}_{\bar{\boldsymbol{\psi}}_2}^\perp(z)$  can be similarly formed from  $\bar{\boldsymbol{\psi}}_2(z)$ ,  $\bar{\mathbf{g}}^H(z)$ , and  $\bar{n}_0$ .

According to (14), a natural estimate of the frequency offset can then be obtained by solving the minimization problem

$$\hat{\omega} = \arg \min_{\omega} \left\{ \left\| \mathbf{P}_{\boldsymbol{\psi}_2}^\perp(z) \boldsymbol{\psi}_1(z) \right\|^2 + \left\| \bar{\mathbf{P}}_{\bar{\boldsymbol{\psi}}_2}^\perp(z) \bar{\boldsymbol{\psi}}_1(z) \right\|^2 \right\} \quad (17)$$

that needs to be minimized for all possible values of  $p$ . Specifically, for  $p = 0, 1, \dots, NQ - 1$ , the authors construct the

<sup>2</sup>Note that  $\boldsymbol{\mu}$  is by construction nontrivial (viz.  $\boldsymbol{\mu} \neq \mathbf{0}$ ) for all possible delays, including when  $\boldsymbol{\mu} = \mathbf{0}$  (i.e., zero fractional delay), for which case it reduces to  $\boldsymbol{\mu} = [1, 0]^T$ .

projection matrices  $\mathbf{P}_{\psi_2}^\perp(z)$  and  $\bar{\mathbf{P}}_{\psi_2}^\perp(z)$  as in the above, and find an estimate  $\hat{\omega}$  by minimizing (17) for each  $p$ ; the final estimate is the one that yields the smallest value of the cost function among the  $NQ$  candidates. For each  $p$ , the minimization of (17) can be efficiently performed by polynomial rooting, similar to the root-MUSIC algorithm [10, p. 158].

Once an estimate of  $\omega$  is known,  $\Psi(z)$  and  $\bar{\Psi}(z)$  are parameterized by the integer delay  $p$ . Then, the authors may write them explicitly as  $\Psi(p)$  and  $\bar{\Psi}(p)$ . It follows from (12) that the following criterion can be used to estimate the integer and fractional delay as

$$\{\hat{p}, \hat{\mu}\} = \arg \min_{p, \mu} \left\{ \|\Psi(p)\boldsymbol{\mu}\|^2 + \|\bar{\Psi}(p)\boldsymbol{\mu}\|^2 \right\}. \quad (18)$$

In the multipath case, there are  $L_k$  solutions corresponding to the  $L_k$  paths of user  $k$ , all achieving identically the same minimum of the cost function, which is zero if  $\mathbf{U}_n$  is known exactly (see discussions next). The authors remark that criterion (18) is equivalent to the one employed in [4, Eq. (23)] for code acquisition assuming no carrier offset. As shown there, it can be efficiently minimized by a sequence of polynomial rooting.

### B. Noisy Case

It can be shown that in the absence of noise, the proposed scheme yields error-free parameter estimates (see, e.g., [10]). With noisy observation, however, (11) no longer holds exactly since only a noisy estimate of  $\mathbf{U}_n$  is available. As a result, the criteria (17) and (18) have to be minimized in the least-squares sense, and the delay and carrier offset estimates are no longer exact. The performance of the proposed scheme in the noisy case is analyzed in Section IV and numerically evaluated in Section VI. The authors briefly summarize the implementation of the proposed scheme as follows.

- 1) Collect all noisy observations and form the data matrix  $\mathbf{Y} \triangleq [\mathbf{y}(0), \dots, \mathbf{y}(M-1)]$ . Compute the SVD of  $\mathbf{Y}$  as

$$\mathbf{Y} = [\hat{\mathbf{U}}_s, \hat{\mathbf{U}}_n] \hat{\boldsymbol{\Lambda}} \hat{\mathbf{V}}^H \quad (19)$$

where  $\hat{\mathbf{U}}_s \in \mathbb{C}^{NQ \times 2L}$  is formed by the  $2L$  left singular vectors associated with  $2L$  largest singular values while  $\hat{\mathbf{U}}_n \in \mathbb{C}^{NQ \times (NQ-2L)}$  collects the rest of the left singular vectors.

- 2) Estimate the carrier offset by (17). Note that the construction of the projection matrices  $\mathbf{P}_{\psi_2}^\perp(z)$  and  $\bar{\mathbf{P}}_{\psi_2}^\perp(z)$ , as well as the minimization of (17) that produces the carrier offset estimate, follows exactly the same way as that described in Section III-A. The only exception is that  $\mathbf{U}_n$  [cf. (13)] is now replaced by the noisy estimate  $\hat{\mathbf{U}}_n$ .
- 3) Estimate the delay by (18), which is minimized as described in Section III-A.

## IV. PERTURBATION ANALYSIS

In the following, an asymptotic expression was derived for the covariance matrix of the carrier offset and the code timing delay estimates obtained by the proposed estimator. The analysis is based on a first-order Taylor expansion of the cost function

involved when the signal-to-noise ratio (SNR) is high. In that case, the parameter estimates deviate slightly from the true values. As such, the Taylor expansion with respect to (w.r.t.)  $\tau_{k,l}$  effectively reduces to the expansion w.r.t. the fractional delay  $\mu_{k,l}$ , assuming knowledge of the integer delay  $p_{k,l}$ . It is noted that (19) and (9) are related as

$$\hat{\mathbf{U}}_n = \mathbf{U}_n + \Delta \mathbf{U}_n$$

where the first-order perturbation is given by [11]

$$\Delta \mathbf{U}_n = -\mathbf{U}_s \boldsymbol{\Lambda}^{-1} \mathbf{V}_s^H \mathbf{N}^H \mathbf{U}_n = -\mathbf{X}^{\dagger H} \mathbf{N}^H \mathbf{U}_n \quad (20)$$

where  $\mathbf{N} \triangleq [\mathbf{n}(0), \dots, \mathbf{n}(M-1)]$ . The cost function to be minimized is

$$J(\omega_k, \mu_{k,l}, \hat{\mathbf{U}}_n) \triangleq \left\| \hat{\mathbf{U}}_n^H \boldsymbol{\Sigma}_k(\omega_k) \mathbf{F}_k(p_{k,l}) \boldsymbol{\mu}_{k,l} \right\|^2 + \left\| \hat{\mathbf{U}}_n^H \boldsymbol{\Sigma}_k(\omega_k) \bar{\mathbf{F}}_k(p_{k,l}) \boldsymbol{\mu}_{k,l} \right\|^2. \quad (21)$$

Hereafter, the subscripts  $k$  and  $l$  and the dependence on  $\omega_k$  and  $\tau_{k,l}$  are sometimes dropped for notational simplicity. Let  $\boldsymbol{\theta} \triangleq [\omega, \mu]^T$ . A first-order Taylor series expansion at  $(\omega, \mu, \hat{\mathbf{U}}_n)$  yields

$$\mathbf{0} = J'(\hat{\omega}, \hat{\mu}, \hat{\mathbf{U}}_n) \approx \mathbf{d}(\omega, \mu, \hat{\mathbf{U}}_n) + \mathbf{H}(\omega, \mu, \hat{\mathbf{U}}_n) \Delta \boldsymbol{\theta} \quad (22)$$

where  $J'(\hat{\omega}, \hat{\mu}, \hat{\mathbf{U}}_n) \triangleq \partial J(\hat{\omega}, \hat{\mu}, \hat{\mathbf{U}}_n) / \partial \boldsymbol{\theta}$ ,  $\mathbf{d}(\omega, \mu, \hat{\mathbf{U}}_n) \triangleq \partial J(\omega, \mu, \hat{\mathbf{U}}_n) / \partial \boldsymbol{\theta}$ , and  $\mathbf{H}(\omega, \mu, \hat{\mathbf{U}}_n)$  denote the Hessian matrix of the cost function evaluated at  $(\omega, \mu, \hat{\mathbf{U}}_n)$ . It follows that

$$\Delta \boldsymbol{\theta} \approx -\mathbf{H}^{-1}(\omega, \mu, \hat{\mathbf{U}}_n) \mathbf{d}(\omega, \mu, \hat{\mathbf{U}}_n). \quad (23)$$

With first-order approximations,  $\mathbf{d}(\omega, \mu, \hat{\mathbf{U}}_n)$  and  $\mathbf{H}(\omega, \mu, \hat{\mathbf{U}}_n)$  can be expressed as

$$\begin{aligned} \mathbf{d}(\omega, \mu, \hat{\mathbf{U}}_n) &= \mathbf{d}(\omega, \mu, \mathbf{U}_n) + \Delta \mathbf{d}(\omega, \mu, \mathbf{U}_n) \\ &= \Delta \mathbf{d}(\omega, \mu, \mathbf{U}_n) \end{aligned} \quad (24)$$

$$\mathbf{H}(\omega, \mu, \hat{\mathbf{U}}_n) = \mathbf{H}(\omega, \mu, \mathbf{U}_n) + \Delta \mathbf{H}(\omega, \mu, \mathbf{U}_n) \quad (25)$$

where the second equality of (24) is due to the fact that  $\mathbf{d}(\omega, \mu, \mathbf{U}_n) = \mathbf{0}$ . Substituting the above equations into (23), the authors have

$$\begin{aligned} \Delta \boldsymbol{\theta} &\approx -[\mathbf{H}^{-1}(\omega, \mu, \mathbf{U}_n) - \mathbf{H}^{-1}(\omega, \mu, \mathbf{U}_n) \Delta \mathbf{H}(\omega, \mu, \mathbf{U}_n) \\ &\quad \times \mathbf{H}^{-1}(\omega, \mu, \mathbf{U}_n)] \Delta \mathbf{d}(\omega, \mu, \mathbf{U}_n) \\ &\approx -\mathbf{H}^{-1}(\omega, \mu, \mathbf{U}_n) \Delta \mathbf{d}(\omega, \mu, \mathbf{U}_n) \end{aligned} \quad (26)$$

where the second-order term was ignored.

The authors now evaluate first-order derivative  $\mathbf{d}(\omega, \mu, \hat{\mathbf{U}}_n)$  and the Hessian matrix  $\mathbf{H}(\omega, \mu, \mathbf{U}_n)$  as follows. Let

$$\begin{aligned}\hat{\boldsymbol{\mu}} &\triangleq \frac{\partial \boldsymbol{\mu}}{\partial \mu} = [-1, 1]^T \\ \hat{\boldsymbol{\Sigma}} &\triangleq \frac{\partial \boldsymbol{\Sigma}}{\partial \omega} = j \operatorname{diag} \left\{ 0, e^{j\omega}, \dots, (NQ-1)e^{j\omega(NQ-1)} \right\} \\ \hat{\boldsymbol{\Sigma}} &\triangleq \frac{\partial^2 \boldsymbol{\Sigma}}{\partial^2 \omega^2} = -\operatorname{diag} \left\{ 0, e^{j\omega}, \dots, (NQ-1)^2 e^{j\omega(NQ-1)} \right\}.\end{aligned}$$

By direct computation, the authors have [using (20) and the fact that  $\mathbf{U}_n^H \boldsymbol{\Sigma} \mathbf{F} \boldsymbol{\mu} = \mathbf{U}_n^H \boldsymbol{\Sigma} \bar{\mathbf{F}} \boldsymbol{\mu} = \mathbf{0}$  and keeping only the first-order terms]

$$\begin{aligned}\frac{\partial J(\omega, \mu, \hat{\mathbf{U}}_n)}{\partial \omega} &= 2\Re \left[ \boldsymbol{\mu}^H \mathbf{F}^H \hat{\boldsymbol{\Sigma}}^H \hat{\mathbf{U}}_n \hat{\mathbf{U}}_n^H \boldsymbol{\Sigma} \mathbf{F} \boldsymbol{\mu} \right. \\ &\quad \left. + \boldsymbol{\mu}^H \bar{\mathbf{F}}^H \hat{\boldsymbol{\Sigma}}^H \hat{\mathbf{U}}_n \hat{\mathbf{U}}_n^H \boldsymbol{\Sigma} \bar{\mathbf{F}} \boldsymbol{\mu} \right] \\ &\approx -2\Re \left[ \boldsymbol{\mu}^H \mathbf{F}^H \hat{\boldsymbol{\Sigma}}^H \mathbf{U}_n \mathbf{U}_n^H \mathbf{N} \mathbf{X}^\dagger \boldsymbol{\Sigma} \mathbf{F} \boldsymbol{\mu} \right. \\ &\quad \left. + \boldsymbol{\mu}^H \bar{\mathbf{F}}^H \hat{\boldsymbol{\Sigma}}^H \mathbf{U}_n \mathbf{U}_n^H \mathbf{N} \mathbf{X}^\dagger \boldsymbol{\Sigma} \bar{\mathbf{F}} \boldsymbol{\mu} \right]\end{aligned}\quad (27)$$

$$\begin{aligned}\frac{\partial J(\omega, \mu, \hat{\mathbf{U}}_n)}{\partial \mu} &= 2\Re \left[ \hat{\boldsymbol{\mu}}^H \mathbf{F}^H \boldsymbol{\Sigma}^H \hat{\mathbf{U}}_n \hat{\mathbf{U}}_n^H \boldsymbol{\Sigma} \mathbf{F} \boldsymbol{\mu} \right. \\ &\quad \left. + \hat{\boldsymbol{\mu}}^H \bar{\mathbf{F}}^H \boldsymbol{\Sigma}^H \hat{\mathbf{U}}_n \hat{\mathbf{U}}_n^H \boldsymbol{\Sigma} \bar{\mathbf{F}} \boldsymbol{\mu} \right] \\ &\approx -2\Re \left[ \hat{\boldsymbol{\mu}}^H \mathbf{F}^H \boldsymbol{\Sigma}^H \mathbf{U}_n \mathbf{U}_n^H \mathbf{N} \mathbf{X}^\dagger \boldsymbol{\Sigma} \mathbf{F} \boldsymbol{\mu} \right. \\ &\quad \left. + \hat{\boldsymbol{\mu}}^H \bar{\mathbf{F}}^H \boldsymbol{\Sigma}^H \mathbf{U}_n \mathbf{U}_n^H \mathbf{N} \mathbf{X}^\dagger \boldsymbol{\Sigma} \bar{\mathbf{F}} \boldsymbol{\mu} \right]\end{aligned}\quad (28)$$

$$\begin{aligned}\frac{\partial^2 J(\omega, \mu, \mathbf{U}_n)}{\partial \omega \partial \mu} &= 2\Re \left[ \boldsymbol{\mu}^H \mathbf{F}^H \hat{\boldsymbol{\Sigma}}^H \mathbf{U}_n \mathbf{U}_n^H \boldsymbol{\Sigma} \mathbf{F} \hat{\boldsymbol{\mu}} \right. \\ &\quad \left. + \boldsymbol{\mu}^H \bar{\mathbf{F}}^H \hat{\boldsymbol{\Sigma}}^H \mathbf{U}_n \mathbf{U}_n^H \boldsymbol{\Sigma} \bar{\mathbf{F}} \hat{\boldsymbol{\mu}} \right]\end{aligned}\quad (29)$$

$$\begin{aligned}\frac{\partial^2 J(\omega, \mu, \mathbf{U}_n)}{\partial \omega^2} &= 2\boldsymbol{\mu}^H \mathbf{F}^H \hat{\boldsymbol{\Sigma}}^H \mathbf{U}_n \mathbf{U}_n^H \boldsymbol{\Sigma} \mathbf{F} \hat{\boldsymbol{\mu}} \\ &\quad + 2\boldsymbol{\mu}^H \bar{\mathbf{F}}^H \hat{\boldsymbol{\Sigma}}^H \mathbf{U}_n \mathbf{U}_n^H \boldsymbol{\Sigma} \bar{\mathbf{F}} \hat{\boldsymbol{\mu}}\end{aligned}\quad (30)$$

$$\begin{aligned}\frac{\partial^2 J(\omega, \mu, \mathbf{U}_n)}{\partial \mu^2} &= 2\hat{\boldsymbol{\mu}}^H \mathbf{F}^H \boldsymbol{\Sigma}^H \mathbf{U}_n \mathbf{U}_n^H \boldsymbol{\Sigma} \mathbf{F} \hat{\boldsymbol{\mu}} \\ &\quad + 2\hat{\boldsymbol{\mu}}^H \bar{\mathbf{F}}^H \boldsymbol{\Sigma}^H \mathbf{U}_n \mathbf{U}_n^H \boldsymbol{\Sigma} \bar{\mathbf{F}} \hat{\boldsymbol{\mu}}.\end{aligned}\quad (31)$$

Substituting (27) and (28) into (26), while observing that the noise is zero mean and independent of the signal part  $\mathbf{X}$ , the authors have  $E\{\Delta \boldsymbol{\theta}\} \approx \mathbf{0}$ , implying that the estimator is asymptotically unbiased. The asymptotic covariance matrix is

$$\begin{aligned}\operatorname{cov}(\boldsymbol{\theta}) &\triangleq E\{\Delta \boldsymbol{\theta} \Delta \boldsymbol{\theta}^H\} \\ &= \mathbf{H}^{-1}(\omega, \mu, \mathbf{U}_n) \mathbf{R}_d \mathbf{H}^{-H}(\omega, \mu, \mathbf{U}_n)\end{aligned}\quad (32)$$

where  $\mathbf{R}_d \triangleq E\{\Delta \mathbf{d}(\omega, \mu, \mathbf{U}_n) \Delta \mathbf{d}^H(\omega, \mu, \mathbf{U}_n)\}$  is computed in Appendix B.

## V. CRB

A CRB that is averaged over unknown user symbols and channel fading is derived herein. Recall (2), which is rewritten as

$$\mathbf{y}(m) \triangleq \boldsymbol{\Theta}(\omega) \mathcal{A}(\boldsymbol{\tau}) \boldsymbol{\beta}(m) + \mathbf{n}(m) \quad m = 0, \dots, M-1. \quad (33)$$

In what follows, the standard assumption that the information symbols, fading, and noise are zero-mean and independent of one another was used. To facilitate arriving at a simple but useful CRB expression, the authors further assume that  $\{\boldsymbol{\beta}(m)\}_{m=0}^{M-1}$  are Gaussian with zero-mean and covariance matrix  $E\{\boldsymbol{\beta}(m_1) \boldsymbol{\beta}^H(m_2)\} = \mathbf{R}_{\beta} \delta(m_1 - m_2)$ , where  $\mathbf{R}_{\beta} \triangleq E\{\boldsymbol{\beta}(m) \boldsymbol{\beta}^H(m)\} = \operatorname{diag}\{\mathbf{R}_{\beta_1}, \dots, \mathbf{R}_{\beta_K}\}$ ,  $E\{\boldsymbol{\beta}_k(m) \boldsymbol{\beta}_k^H(m)\} = \operatorname{diag}\{P_{k,1}, P_{k,1}, \dots, P_{k,L_k}, P_{k,L_k}\}$ , with  $P_{k,l} \triangleq E\{|\alpha_{k,l}(m)|^2\}$  denoting the average power of the  $l$ th path of user  $k$  and  $\delta(n)$  denoting the Kronecker delta. It is noted that the CRB based on a Gaussian assumption is the lower bound for the covariance matrices of a large class of estimation methods, regardless of the data distribution [10, p. 293]. Let  $\mathbf{y} \triangleq [\mathbf{y}^T(0), \dots, \mathbf{y}^T(M-1)]^T$ . With the above assumptions, it is easy to show that  $\mathbf{y}$  is Gaussian with zero-mean and covariance  $\mathbf{I}_M \otimes \mathbf{R}_y$ , where

$$\mathbf{R}_y \triangleq \boldsymbol{\Theta}(\omega) \mathcal{A}(\boldsymbol{\tau}) \mathbf{R}_{\beta} \mathcal{A}(\boldsymbol{\tau})^H \boldsymbol{\Theta}^H(\omega) + \sigma_n^2 \mathbf{I}.$$

Let  $\boldsymbol{\phi}$  collect all unknown parameters

$$\boldsymbol{\phi} \triangleq [\boldsymbol{\phi}_{\tau}^T, \boldsymbol{\phi}_{\omega}^T, \boldsymbol{\phi}_P^T, \sigma_n^2]^T$$

where  $\boldsymbol{\phi}_{\tau} \triangleq [\boldsymbol{\tau}_1^T, \dots, \boldsymbol{\tau}_K^T]^T$ ,  $\boldsymbol{\phi}_{\omega} \triangleq [\omega_1, \dots, \omega_K]^T$ , and  $\boldsymbol{\phi}_P \triangleq [P_{1,1}, \dots, P_{1,L_1}, \dots, P_{K,1}, \dots, P_{K,L_K}]^T$ , and  $\sigma_n^2$  denotes the noise variance. By the Slepian–Bangs formula, the CRB matrix is given element-wise by (e.g., [10])

$$[\operatorname{CRB}^{-1}(\boldsymbol{\phi})]_{i,j} = M \operatorname{tr} \left[ \mathbf{R}_y^{-1} \frac{\partial \mathbf{R}_y}{\partial [\boldsymbol{\phi}]_i} \mathbf{R}_y^{-1} \frac{\partial \mathbf{R}_y}{\partial [\boldsymbol{\phi}]_j} \right]. \quad (34)$$

The partial derivatives are computed as

$$\begin{aligned}\frac{\partial \mathbf{R}_y}{\partial \tau_{k,l}} &= P_{k,l} \boldsymbol{\Sigma}_k(\omega_k) \left[ \mathbf{F}_k(p_{k,l}) \mathbf{D}_{k,l} \mathbf{F}_k^H(p_{k,l}) \right. \\ &\quad \left. + \bar{\mathbf{F}}_k(p_{k,l}) \mathbf{D}_{k,l} \bar{\mathbf{F}}_k^H(p_{k,l}) \right] \boldsymbol{\Sigma}_k^H(\omega_k)\end{aligned}\quad (35)$$

$$\begin{aligned}\frac{\partial \mathbf{R}_y}{\partial \omega_k} &= P_{k,l} \boldsymbol{\Sigma}_k(\omega_k) \left[ \mathbf{a}_k(\tau_{k,l}) \mathbf{a}_k^H(\tau_{k,l}) \right. \\ &\quad \left. + \bar{\mathbf{a}}_k(\tau_{k,l}) \bar{\mathbf{a}}_k^H(\tau_{k,l}) \right] \hat{\boldsymbol{\Sigma}}_k^H(\omega_k) \\ &\quad + P_{k,l} \hat{\boldsymbol{\Sigma}}_k(\omega_k) \left[ \mathbf{a}_k(\tau_{k,l}) \mathbf{a}_k^H(\tau_{k,l}) \right. \\ &\quad \left. + \bar{\mathbf{a}}_k(\tau_{k,l}) \bar{\mathbf{a}}_k^H(\tau_{k,l}) \right] \boldsymbol{\Sigma}_k^H(\omega_k)\end{aligned}\quad (36)$$

$$\begin{aligned}\frac{\partial \mathbf{R}_y}{\partial P_{k,l}} &= \boldsymbol{\Sigma}_k(\omega_k) \left[ \mathbf{a}_k(\tau_{k,l}) \mathbf{a}_k^H(\tau_{k,l}) \right. \\ &\quad \left. + \bar{\mathbf{a}}_k(\tau_{k,l}) \bar{\mathbf{a}}_k^H(\tau_{k,l}) \right] \boldsymbol{\Sigma}_k^H(\omega_k)\end{aligned}\quad (37)$$

where

$$\mathbf{D}_{k,l} = \begin{bmatrix} 2(\mu_{k,l} - 1) & 1 - 2\mu_{k,l} \\ 1 - 2\mu_{k,l} & 2\mu_{k,l} \end{bmatrix}$$

$$\hat{\Sigma}_k(\omega_k) = j \text{diag} \left\{ 0, e^{j\omega_k}, \dots, (NQ - 1)e^{j\omega_k(NQ-1)} \right\}.$$

Finally, the partial differentiation w.r.t the noise variance is given by

$$\frac{\partial \mathbf{R}_y}{\partial \sigma_n^2} = \mathbf{I}_{NQ}.$$

Substituting this last equation, along with (35)–(37), in (34), the CRB can be readily calculated.

### VI. NUMERICAL RESULTS

The authors consider a  $K$ -user asynchronous DS-CDMA system using binary phase-shift keying (BPSK) and  $N = 15$  large Kasami spreading codes [1] in frequency-selective time-varying Rayleigh fading channels. The fading  $\alpha_{k,l}(t)$  [cf. (1)] is generated by the model of [12], parameterized by the normalized Doppler rate  $f_D T_s$ , where  $f_D$  is the maximum Doppler rate. The fading is updated continuously for every sampling interval  $T_s$ . To model both small- and large-scale fading, the authors use  $\alpha_{k,l}(i) = \gamma_{k,l}(i)P_{k,l}$ , where  $i$  is the sampling index,  $\gamma_{k,l}(i) \sim \mathcal{CN}(0,1)$  models the small-scale Rayleigh fading, generated according to the Jakes' model, while  $P_{k,l}$  follows a log normal distribution to emulate the large-scale path loss and shadowing. The authors consider near-far environments, where the total (from all paths) average power for the desired user is scaled so that  $P_1 \triangleq \sum_{l=1}^{L_1} P_{1,l} = 1$ , while the mean power for the  $K - 1$  interfering is  $\bar{P}$  decibel (referred to as the near-far ratio or NFR) higher than that of the desired user. The average SNR for the desired user is defined as  $\text{SNR} \triangleq NQ/\sigma_n^2$ . In all examples, the authors use  $f_D T_s = 0.0067$ ,  $\omega_k = 0.1$  for the desired user, and the time delays are generated randomly and fixed for all users (to facilitate comparison with the CRB). The authors compare the proposed estimator and the MD-Search based scheme (10) (also see [7]). The latter is initialized by estimates obtained by the method in [4], assuming zero initial carrier offset, and then iterates using the Matlab function `fminsearch` till convergence. Two performance measures are considered. The first is the probability of correct acquisition (PCA), defined as the probability of the event that the code timing estimation error is less than  $T_c/2$ . The second is the root-mean-squared error (rmse) of parameter estimates obtained from all simulation runs.<sup>3</sup>

The authors first consider changing the SNR in time-varying two-path Rayleigh fading channels. The simulation parameters are  $K = 5$ ,  $M = 200$ ,  $Q = 2$ , and NFR = 10 dB. The PCA of the two methods is shown in Fig. 1(a). The MD-Search scheme is seen to suffer local convergence caused by poor initialization, yielding a lower PCA. Fig. 1(b) depicts the rmse

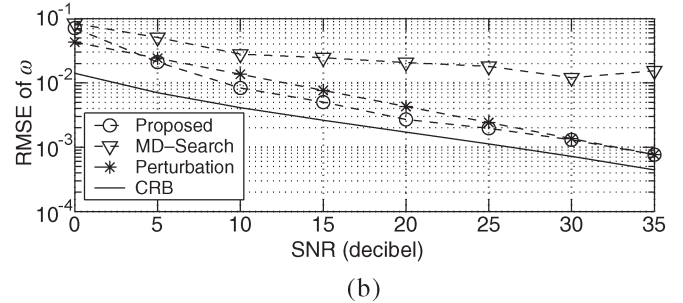
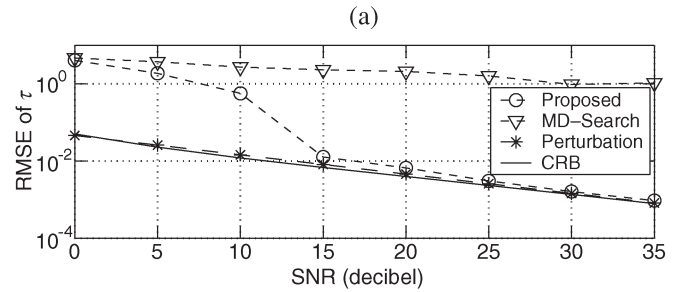
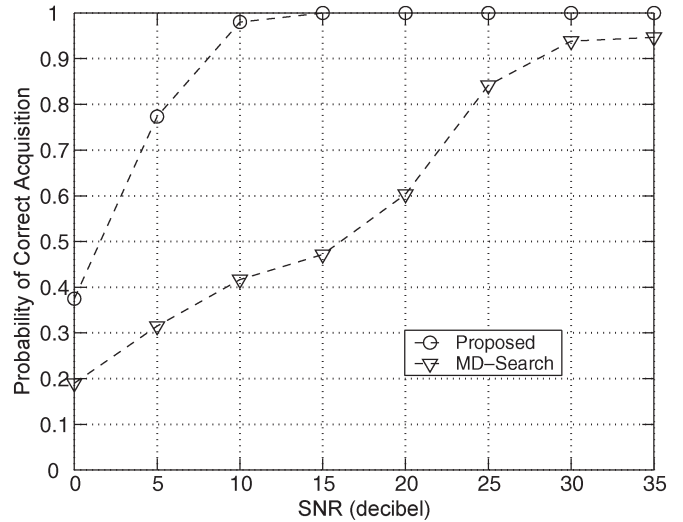


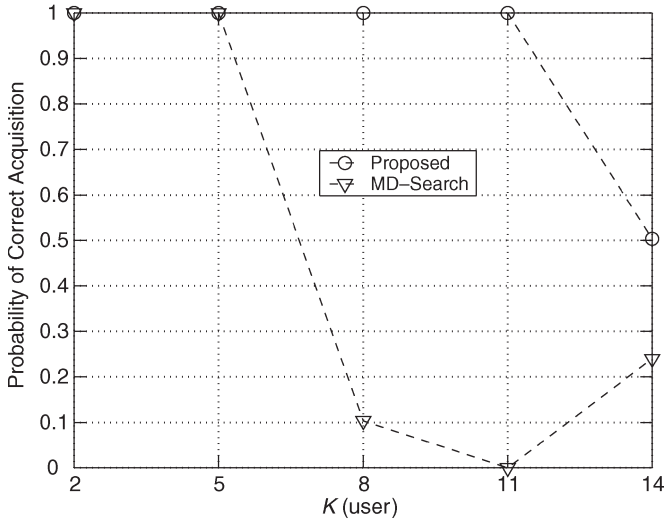
Fig. 1. Performance versus SNR in a time-varying two-path fading channel when  $M = 200$ ,  $Q = 2$ ,  $K = 5$ ,  $N = 15$ , and NFR = 10 dB. (a) PCA. (b) rmse of  $\tau$  (top) and  $\omega$  (bottom).

of the parameter estimates along with the perturbation analysis result and the CRB. Note that the rmse results are obtained by averaging all Monte Carlo runs. As the SNR increases, it is seen that the rmse of the proposed scheme and the perturbation analysis are very close to each other. It is also seen that the proposed scheme approaches the CRB as SNR increases.

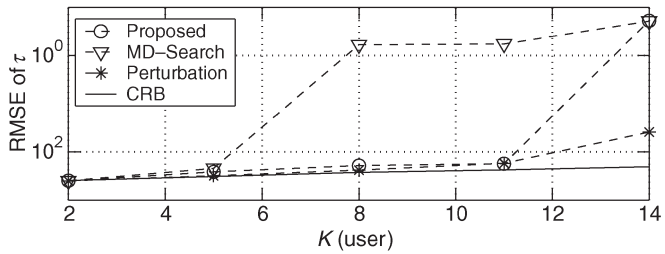
Next, user capacity is examined, i.e., the number of users that can be supported. The setup is similar to the first example except that SNR = 20 dB and the channel is flat fading. The results are depicted in Fig. 2(a) and (b). It is noted that the proposed scheme achieves a larger user capacity and gives a better performance.

Finally, the authors consider the effect of  $M$ , i.e., the number of data symbols used for synchronization, when  $K = 5$ ,  $Q = 2$ , SNR = 20 dB, and NFR = 10 dB in time-varying two-path Rayleigh fading channels. The results are depicted in Figs. 3(a) and (b). It is seen that the number of symbols required by the proposed scheme is relatively small.

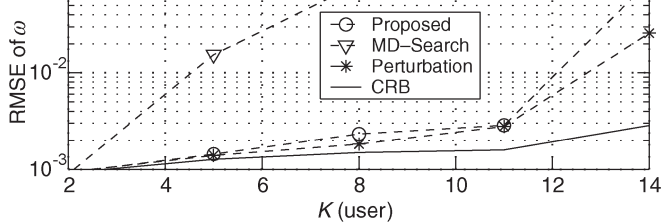
<sup>3</sup>For multipath propagation, the authors report the PCA and RMSE of the delay estimates averaged over all paths for the desired user.



(a)



(b)



(b)

Fig. 2. Performance versus number of users  $K$  in a time-varying flat-fading channel when  $Q = 2$ ,  $M = 200$ ,  $N = 15$ ,  $\text{SNR} = 20$  dB, and  $\text{NFR} = 10$  dB. (a) PCA. (b) rmse of  $\tau$  (top) and  $\omega$  (bottom).

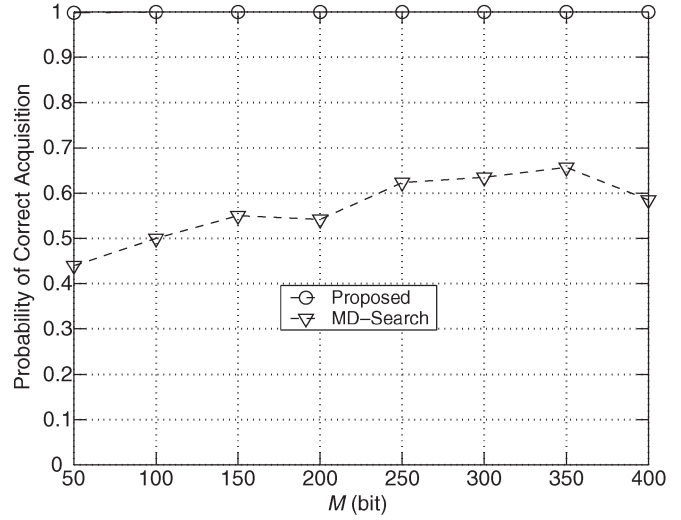
VII. CONCLUSION

The authors have presented an algebraic blind joint carrier offset and code timing estimation algorithm for direct-sequence code-division multiple-access (DS-CDMA) systems. The performance of the proposed scheme has been examined analytically by a first-order perturbation analysis. An unconditional Cramér–Rao bound (CRB) for the estimation problem has also been derived. Numerical results show that the proposed estimator performs well in near–far time-varying multipath fading channels, and the analysis agrees well with simulation at high signal-to-noise ratio (SNR).

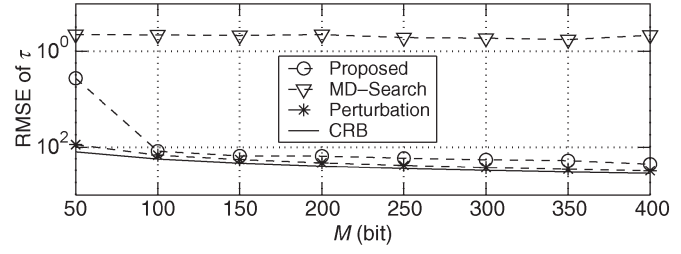
APPENDIX A

CONSTRUCTION OF  $\mathbf{g}^H(z)$  AND  $\bar{\mathbf{g}}^H(z)$

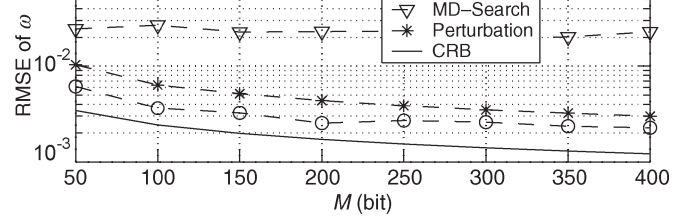
Here, the authors show how to construct  $\mathbf{g}^H(z)$ ;  $\bar{\mathbf{g}}^H(z)$  follows exactly the same way.  $\psi_2(z)$  and  $\mathbf{g}^H(z)$  are first



(a)



(b)



(b)

Fig. 3. Performance versus number of bits  $M$  in a time-varying two-path fading channel when  $Q = 2$ ,  $K = 5$ ,  $N = 15$ ,  $\text{SNR} = 20$  dB, and  $\text{NFR} = 10$  dB. (a) PCA. (b) rmse of  $\tau$  (top) and  $\omega$  (bottom).

expressed explicitly as polynomial vectors

$$\psi_2(z) = \sum_{i=0}^{NQ-1} \psi_{2,i} z^i, \quad \mathbf{g}^H(z) = \sum_{i=0}^{B-1} \mathbf{g}_i^H z^{-i}.$$

Let  $\mathbf{g}^H = [\mathbf{g}_{B-1}^H, \dots, \mathbf{g}_0^H]_{1 \times B(NQ-2L)}$ .  $B$  was chosen such that  $B > (NQ - 1)/(NQ - 2L - 1)$  to ensure that the matrix  $\Upsilon$  is tall as

$$\Upsilon \triangleq \begin{bmatrix} \psi_{2,0} & \cdots & \psi_{2,NQ-1} & & \mathbf{0} \\ & & & \ddots & \\ \mathbf{0} & & \psi_{2,0} & \cdots & \psi_{2,NQ-1} \end{bmatrix}. \quad (38)$$

Then, the convolution of (15) can be represented by  $\mathbf{g}^H \Upsilon = \mathbf{e}_{n_0}^T$ , where  $\mathbf{e}_{n_0}$  denotes a unit vector that contains a unit element at the  $n_0$ th location and zeros elsewhere. As shown

in [8], there exist block vector  $\mathbf{g}^H$  satisfying the above equations if and only if the product  $\mathbf{Y}^\dagger \mathbf{Y}$  has the form

$$\begin{bmatrix} * & \mathbf{0} & * \\ \mathbf{0} & 1 & \mathbf{0} \\ * & \mathbf{0} & * \end{bmatrix} \quad (39)$$

where  $*$  stands for any value. Therefore, the delay  $n_0$  can be chosen such that the  $n_0$ th diagonal element of  $\mathbf{Y}^\dagger \mathbf{Y}$  is equal to 1. In general, the choice of the delay  $n_0$  is not unique. In the ideal noise-free case, any valid choices will give identical results. In the presence of noise, however, the choice of  $n_0$  becomes more critical, and different delays can lead to different results. To find the best  $n_0$ , it can be selected as the one yielding the smallest values of the cost function. Once  $n_0$  is determined,  $\mathbf{g}^H$  can be calculated as [8]  $\mathbf{g}^H = \mathbf{e}_{n_0}^T \mathbf{Y}^\dagger$ , from which the authors can readily construct  $\mathbf{g}^H(z)$ .

#### APPENDIX B CALCULATION OF $\mathbf{R}_d$

For notational convenience, let

$$\Delta \mathbf{d}(\omega, \mu, \mathbf{U}_n) \triangleq [\Delta d_\omega, \Delta d_\mu]^T$$

where

$$\Delta d_\omega \triangleq \frac{\partial J(\omega, \mu, \hat{\mathbf{U}}_n)}{\partial \omega}, \quad \Delta d_\mu \triangleq \frac{\partial J(\omega, \mu, \hat{\mathbf{U}}_n)}{\partial \mu}$$

that are given in (27) and (28), respectively. Then,  $\mathbf{R}_d = \begin{bmatrix} R_\omega & R_{\omega, \mu} \\ R_{\omega, \mu} & R_\mu \end{bmatrix}$ , where  $R_\omega \triangleq E\{(\Delta d_\omega)^2\}$ ,  $R_\mu \triangleq E\{(\Delta d_\mu)^2\}$ ,  $R_{\omega, \mu} \triangleq E\{\Delta d_\omega \Delta d_\mu\}$ , and note that  $\mathbf{R}_d$  is a real symmetric matrix. Direct calculations using (27) and (28) followed by simplifications yield

$$R_\omega = 2\sigma_n^2 \Re [\rho_1 \boldsymbol{\mu}^H \mathbf{F}^H \boldsymbol{\Xi}_1 \mathbf{F} \boldsymbol{\mu} + \rho_2 \boldsymbol{\mu}^H \mathbf{F}^H \boldsymbol{\Xi}_1 \bar{\mathbf{F}} \boldsymbol{\mu} + \rho_2^* \boldsymbol{\mu}^H \bar{\mathbf{F}}^H \boldsymbol{\Xi}_1 \mathbf{F} \boldsymbol{\mu} + \rho_3 \boldsymbol{\mu}^H \bar{\mathbf{F}}^H \boldsymbol{\Xi}_1 \bar{\mathbf{F}} \boldsymbol{\mu}] \quad (40)$$

$$R_\mu = 2\sigma_n^2 \Re [\rho_1 \hat{\boldsymbol{\mu}}^H \mathbf{F}^H \boldsymbol{\Xi}_2 \mathbf{F} \hat{\boldsymbol{\mu}} + \rho_2 \hat{\boldsymbol{\mu}}^H \mathbf{F}^H \boldsymbol{\Xi}_2 \bar{\mathbf{F}} \hat{\boldsymbol{\mu}} + \rho_2^* \hat{\boldsymbol{\mu}}^H \bar{\mathbf{F}}^H \boldsymbol{\Xi}_2 \mathbf{F} \hat{\boldsymbol{\mu}} + \rho_3 \hat{\boldsymbol{\mu}}^H \bar{\mathbf{F}}^H \boldsymbol{\Xi}_2 \bar{\mathbf{F}} \hat{\boldsymbol{\mu}}] \quad (41)$$

$$R_{\omega, \mu} = 2\sigma_n^2 \Re [\rho_1 \boldsymbol{\mu}^H \mathbf{F}^H \boldsymbol{\Xi}_3 \mathbf{F} \hat{\boldsymbol{\mu}} + \rho_2 \boldsymbol{\mu}^H \mathbf{F}^H \boldsymbol{\Xi}_3 \bar{\mathbf{F}} \hat{\boldsymbol{\mu}} + \rho_2^* \boldsymbol{\mu}^H \bar{\mathbf{F}}^H \boldsymbol{\Xi}_3 \mathbf{F} \hat{\boldsymbol{\mu}} + \rho_3 \boldsymbol{\mu}^H \bar{\mathbf{F}}^H \boldsymbol{\Xi}_3 \bar{\mathbf{F}} \hat{\boldsymbol{\mu}}] \quad (42)$$

where

$$\rho_1 = \boldsymbol{\mu}^H \mathbf{F}^H \boldsymbol{\Sigma}^H \mathbf{X}^{\dagger H} \mathbf{X}^\dagger \boldsymbol{\Sigma} \mathbf{F} \boldsymbol{\mu}$$

$$\rho_2 = \boldsymbol{\mu}^H \bar{\mathbf{F}}^H \boldsymbol{\Sigma}^H \mathbf{X}^{\dagger H} \mathbf{X}^\dagger \boldsymbol{\Sigma} \mathbf{F} \boldsymbol{\mu}$$

$$\rho_3 = \boldsymbol{\mu}^H \bar{\mathbf{F}}^H \boldsymbol{\Sigma}^H \mathbf{X}^{\dagger H} \mathbf{X}^\dagger \boldsymbol{\Sigma} \bar{\mathbf{F}} \boldsymbol{\mu}$$

$$\boldsymbol{\Xi}_1 = \boldsymbol{\Sigma}^H \mathbf{U}_n \mathbf{U}_n^H \boldsymbol{\Sigma}$$

$$\boldsymbol{\Xi}_2 = \boldsymbol{\Sigma}^H \mathbf{U}_n \mathbf{U}_n^H \boldsymbol{\Sigma}$$

$$\boldsymbol{\Xi}_3 = \boldsymbol{\Sigma}^H \mathbf{U}_n \mathbf{U}_n^H \boldsymbol{\Sigma}.$$

In carrying out the above calculations, the authors used the fact that the noise is a complex white Gaussian with zero-mean and variance  $\sigma_n^2$ , which implies that  $E\{\mathbf{a}^H \mathbf{N} \mathbf{b} \mathbf{c}^H \mathbf{N} \mathbf{d}\} = 0$  and  $E\{\mathbf{a}^H \mathbf{N} \mathbf{b} \mathbf{c}^H \mathbf{N}^H \mathbf{d}\} = \sigma_n^2 \mathbf{a}^H \mathbf{d} \mathbf{c}^H \mathbf{b}$  for arbitrary vectors  $\mathbf{a}$ ,  $\mathbf{b}$ ,  $\mathbf{c}$ , and  $\mathbf{d}$  of proper dimensions.

#### REFERENCES

- [1] R. L. Peterson, R. E. Ziemer, and D. E. Borth, *Introduction to Spread Spectrum Communications*. Englewood Cliffs, NJ: Prentice-Hall, 1995.
- [2] R. F. Smith and S. L. Miller, "Acquisition performance of an adaptive receiver for DS-SS-SSMA," *IEEE Trans. Commun.*, vol. 47, no. 9, pp. 1416–1424, Sep. 1999.
- [3] H. Li, J. Li, and S. L. Miller, "Decoupled multiuser code-timing estimation for code-division multiple-access communication systems," *IEEE Trans. Commun.*, vol. 49, no. 8, pp. 1425–1436, Aug. 2001.
- [4] E. G. Ström, S. Parkvall, S. L. Miller, and B. E. Ottersten, "Propagation delay estimation in asynchronous direct-sequence code-division multiple access systems," *IEEE Trans. Commun.*, vol. 44, no. 1, pp. 84–93, Jan. 1996.
- [5] S. E. Bensley and B. Aazhang, "Subspace-based channel estimation for code division multiple access communications systems," *IEEE Trans. Commun.*, vol. 44, no. 8, pp. 1009–1020, Aug. 1996.
- [6] H. Li and R. Wang, "Filterbank-based blind code synchronization for DS-SS-SSMA systems in multipath fading channels," *IEEE Trans. Signal Process.*, vol. 51, no. 1, pp. 160–161, Jan. 2003.
- [7] M. Erić and M. Obradović, "Subspace-based joint time-delay and frequency-shift estimation in asynchronous systems," *Electron. Lett.*, vol. 33, no. 14, pp. 1193–1195, Jul. 1997.
- [8] K. Li and H. Liu, "Joint channel and carrier offset estimation in CDMA communications," *IEEE Trans. Signal Process.*, vol. 47, no. 7, pp. 1811–1822, Jul. 1999.
- [9] T. Kailath, *Linear Systems*. Englewood Cliffs, NJ: Prentice-Hall, 1980.
- [10] P. Stoica and R. L. Moses, *Introduction to Spectral Analysis*. Upper Saddle River, NJ: Prentice-Hall, 1997.
- [11] F. Li, H. Liu, and R. J. Vaccaro, "Performance analysis for DOA estimation algorithms: Further unification, simplification, and observations," *IEEE Trans. Aerosp. Electron. Syst.*, vol. 29, no. 4, pp. 1170–1184, Oct. 1993.
- [12] W. C. Jakes, Jr., *Microwave Mobile Communications*. New York: Wiley-Interscience, 1974.